Grade 3D Block Modeling and Reserve Estimation of the C-North Iron Skarn Ore Deposit, Sangan, NE Iran

Ali Rezaei[1], Hossein Hassani[1,*], Parviz Moarefvand[1] and Abbas Golmohammadi[2]

[1]Department of Mining and Metallurgical Engineering, Amirkabir University of Technology, Tehran, Iran

[2]Geological Survey and Mineral Exploration of Iran, Tehran, Iran

Abstract: Estimation of ore grade is a time and cost consuming process that requires laboratory-based and exploratory information to present the shape and the ore grade distribution of ore deposit in three dimensional space. The block size is one of the most important parameters which impacts the quality of grade estimates in a resource model. This study aims at spatial modeling of iron ore deposit using geostatistical estimation methods such as Ordinary Kriging based on error estimation, selection of the appropriate size for mining blocks using Vlse Kriterijumsk Optimizacija Kompromisno Resenje method, and performing a three-dimensional block modeling along a grade estimation study for the resource estimation in the C-North iron ore deposit, NE Iran. The variogram that was used in OK estimation was cross validated. Cross validation results showed that compared with the local model, OK with the global model was the most appropriate model for the ore body. Detailed distribution maps of total iron contents in the C-North ore deposit showed a close relationship between structural features and higher iron contents, relative to other areas of the ore deposit. Structural features included the major faults and fault zones along the axial plane. These structures are interpreted to have played a significant role in (re) mobilisation and concentration of the metals, in agreement with observations made elsewhere in the Sangan iron ore complex. Based on the estimation results, 83 million tons of resource was estimated at an average grade of 41.86 % Fe using OK method. The C-North ore deposit has been classified based on the relative estimation error variance and the Australasian Code for Reporting of Mineral Resources and Ore Reserves. It is hoped that this example, taken from very different application fields, will encourage practitioners in applying an OK method with variety of ore deposits.

Keywords: Grade estimation, Block modeling, Ordinary Kriging, VIKOR, Sangan, Iran.

1. INTRODUCTION

A critical task of any mining project is to construct a three-dimensional block model mainly representing the tonnage and grade distribution of the mineralized deposit. Occurrences and distributions of the iron ores have gotten attention in mapping and grade-wise categorization of different types of iron ores. The use of three-dimensional (3D) modeling is inevitable to estimate the exact amount of the deposit as well as in detailed planning for mining and ore production [1]. 3D modeling can be effective in control of mineral mixing in different sectors in addition to consideration of the production plan. Also, a good knowledge of grade distribution within an ore deposit is essential to assess the economic feasibility of mine production [2]. The success in a mining operation depends on the accuracy of the reserves evaluation as well as the distribution of ore grades of the individual blocks [3]. A two-dimensional (2D) or 3D computerized model of the grade distribution is fundamental to modern mineral resource estimation through which one can delineate both low and high grade areas. Open pit mine planning and design is traditionally based on a block model of the ore body built by using interpolation techniques, either traditionally such as inverse distance, nearest neighborhood, etc. or through application of geostatistical methods like simple kriging, ordinary kriging, etc., from the drill hole sample data [4]. Geostatistical tools have been considered as powerful techniques for the spatial modeling of the ore deposits, predicting spatial attributes, and quantifying the uncertainty. Geostatistical approaches can be used to investigate the spatial behavior of a variable. Over the past 30 years, geostatistics has became the most established methodology for grade estimation. Various researchers have applied geostatistical methods and successfully modeled the spatial variability of the grade of elements associated with iron ore deposits [2,3,5-10].

Grade estimation is one of the most important stages in reserve calculations [11]. Grade estimation helps to obtain grade-tonnage curves that are used for the prediction of mining production. Estimation of ore grade can be improved by reducing the variance of estimation, which leads to reduction in the regression effect. The ore grade distribution in mineral deposit based on the economic cut-offs should be placed on selective mining units and not sample grades [3]. To decrease the risk of mining activities, geostatistical estimation methods are used to provide an estimation of different regional variables (e.g. grade) in 2D and 3D environments [12-15]. One of the best methods for estimation of different regional variables in ore grade modeling is kriging. Kriging is a linear regression method for estimating point values (or spatial averages) at any location of a region. Kriging, as a group of geostatistical methods, is an interpolation technique that considers both the degree of variation and the distance between known data points in

*Address correspondence to this author at the Department of Mining and Metallurgical Engineering, Amirkabir University of Technology, Tehran, Iran; Tel: +98 2164542945; Fax: +98 2166405846; E-mail: hhassani@aut.ac.ir

E-ISSN: 2409-5710/19

estimating the values in unknown areas [6,16]. Mineral inventories are based on assessing the grades and tonnages through an estimation in the mining industry and one of the most important of them is ordinary kriging (OK). This allows the construction of a model where block grades are estimated, usually from exploratory data. The question now is how much you can trust the proposed reserve based on the geostatistical methods. With initiatives to establish international standards for classifying mineral resources and reserves, it is important to establish the level of confidence in the results and correctly assess the error. For this reason, using the parameters that can be obtained through geostatistical methods, the quantification of exploratory blocks is made that is one of the needs and strengths of this research. Block modeling, representation of an ore body, is one of the most important steps through which the mineral deposit is divided into a series of separate blocks. The grade of the block is estimated by mathematical methods, such as geostatistical interpolation. In this work, we focus on the evaluation and classification of mineral resources by using different methods. Three dimensional modelling of grade in an ore deposit has a lot of advantages. Therefore, if this process is done carefully, evaluations and judgments about different parts of the ore deposit would be better. An important problem in the block modeling in a deposit is the determination of optimum block sizes [7]. Recognition of the ore grade distribution and the block size in each zone will help to decrease the risk of exploration and planning for further mining activities [17,18]. Thus, the block size is the most important concepts in optimal open pit design [1]. Ore grade estimation in smaller blocks is far more difficult than larger blocks, because bases with larger size have lower variability as shown in the central limit theorem. Moreover, the higher the grade distribution in a deposit, the less accurate the grade estimate in it [19]. More recently, multi-criteria decision-making methods such as AHP, TOPSIS, ELECTRE, and VIKOR have been used alone or in combination with fuzzy logic to solve mining problems [19]. The tonnage, average grade, and cutoff are the basic parameters in mineral resource assessments and mining operations [20]. The distributions and relationships of the tonnage- grade and cutoff have been studied for decades to predict resources at a regional scale.

This research focuses on determining the ore zones in the sub-surface environment, spatial modeling of C-North iron ore deposit using geostatistical estimation methods such as OK, selecting the appropriate size of mining blocks using Vlse Kriterijumsk Optimizacija Kompromisno Resenje (VIKOR) method, and 3D block modeling of ore grades. Also, the C-North ore deposit has been classified based on the relative estimation error variance and the Australasian Code for Reporting of Mineral Resources and Ore Reserves (JORC).

2. MATERIALS AND METHODS

2.1. Sangan District

The Sangan iron skarn complex is one of the most important deposits associated with the Tertiary volcanic-plutonic magmatism in NE Iran. The study area is located in SE of the Khorasan-e-Razavi province, approximately 280 km from the City of Mashhad, and in the end part of the Khaf-Kashmar-Bardskan Tertiary magmatic belt of the Central Iran blocks along the regional E-W trending and the eastern segment of large scale old Dorouneh fault passing near the area (Figure **1a**) [21]. This belt is one of the most important economic mineral districts in NE Iran. The Sangan Magmatic Complex (SMC), at the NE edge of the Lut block, includes a thick pile of volcanic rocks intruded by younger granitoid stocks [22]. There are a number of iron ore deposits with considerable reserve amounts in the study area while the iron ore bodies are distributed along the contact zone between the Jurassic clastic rocks or Cretaceous carbonates and the Eocene igneous rocks [23]. These deposits, together with other smaller satellite deposits and occurrences, form a long E-W trending magnetite rich belt. Based on the characteristics of ore deposits, this mining region is divided into western (subdivided into A, A', B, CS (C-South), and CN (C-North)), central (subdivided into Baghak (BA) and Dardvey (D)) anomalies (Figure **1b**) and eastern anomaly (subdivided into Senjedak 1, 2, 3; Madanjoo, Som–Ahanai and Ferezneh).

2.2. Geological Setting of the Study Area

SMC is located in the eastern part of the Sabzevar Dorouneh Magmatic Belt (SDMB). This formation consists of intermediate to felsic intrusive and extrusive (volcanic and pyroclastic) rocks, and is located at the eastern edge of the Khaf- Kashmar- Bardskan Volcano- Plutonic and Tertiary Metallogenic Belt (KKB-VPMB) in NE Iran [24]. The geology of this belt mainly includes Cenozoic silicic to mafic volcanic rocks, which have been intruded by granitoid units of granitic to dioritic composition [23].

The oldest geologic units in the Sangan region include Precambrian schist and Paleozoic metamorphic rocks, which are overlain by a complex assemblage of Eocene volcanics, Oligo-Miocene sedimentary deposits and Jurassic and Cretaceous formations (Figure **1b**). The metasedimentary rocks represent the oldest rock units. The oldest unit is a thick pile (1500 m) of sedimentary rocks that consists

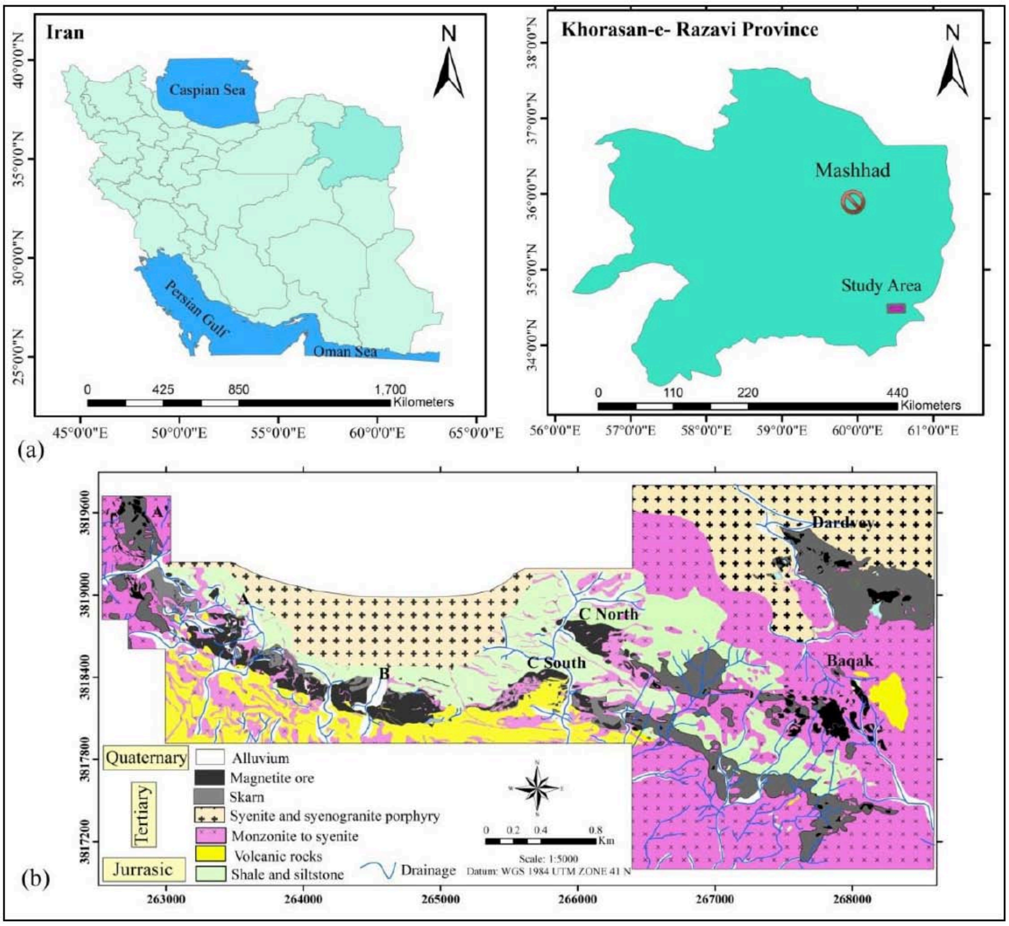

Figure 1: (**a**) Geographic location of the study area; (**b**) Geological map of the Sangan deposits (faults are not shown) (modified after [21, 27]).

of lower Jurassic shales and siltstones, which are overlain by Upper Jurassic to Cretaceous limestone, dolomite and rare gypsum [25]. The whole rock sequence up to the upper Eocene is intruded by Late Eocene granitoids [23]. The carbonate rocks of Jurassic consist of crystalline and less dark dolomite limestone that spread all over the area [26,27]. This sedimentary sequence is either intruded by granitoids or is unconformably covered by the volcanic rocks. The depressions between the ranges are filled in by thick Neogene sediments [28]. Granitoid rock intruded older rocks such as crystalline limestone, dolomite and volcano-sedimentary rocks in the pre-carbonifer age, and quartzite, slate and conglomerate in the carbonifer age. Granites and syenogranites are two main intrusive rocks exposed in the study area [24]. Syenogranites are widespread in the north of the SMC and exhibit porphyritic textures with weak alteration consisting of sericite and chlorite [22]. The structural features of the region such as the faults and foldings as well as the strike of the formations follow the E-W to NW-SE direction of the major Dorouneh fault [21]. The recognition of a fault system and structural features are important because these may materially affect the assessment and exploration of other segments of the hidden ore body. Mineralization and magmatism were controlled by basement-hosted E-W and NW-SE trending fault sets. All of the deposits in the study area are thought to have hydrothermal origins and have skarn type mineralization [29, 30].

2.3. Grade Estimation Geostatistical Methods

Ore grade estimation is one of the most key and complicated aspects in the evaluation of a mineral deposit [31]. The main aim of grade modeling is at providing a quantitative definition of the variables distributed in space [32]. An important problem in mineral exploration is the estimation of mineral resources and reserves of 2D or 3D ore grade distribution with low values of error. In the mining industry, the geostatistical methods, such as kriging, are widely used to predict the value of a whole section based on the sub-surface data. The geostatistical methods provide quick and reliable estimates with minimum variance. On the other hand, geostatistical estimation of the ore grade is necessary in mine planning and designing [33,34]. The choice of estimation method applied depends on the appropriateness of the method to the deposit's geology and the available data. Kriging is used as an unbiased linear estimate of point values (point kriging) or block averages (block kriging) with minimum error variance

[35]. Different variants of kriging estimators have been developed depending on the available source of information and spatial variability of the variable in question [36]. Kriging provides the best estimate since it provides the smallest standard error; narrowest confidence interval and the most confidence (lowest risk) [37]. Kriging utilizes a variogram, which does not depend on the actual value of the variable (data), rather its spatial distribution and internal spatial structure. The variogram provides penetrating insight concerning the data used to construct a kriging interpolation system. When a good robust variogram model is available, kriging provides the estimation best representing the spatial distribution of the input data [5].

2.3.1. Ordinary Kriging

Ordinary Kriging (OK) is an appropriate geostatistical approach and a popular geostatistical method for the estimation of the ore grade and is the most useful technique among different kriging methods, which plays a superior role because of its compatibility with a stationary model that contains a variogram [38,39]. OK, as a linear estimation method, instead of weighting nearby data points by some power of their inverted distance, relies on the spatial correlation structure of the data to determine the weighting values. This is a more rigorous approach to modelling as spatial correlation between the data points determines the estimated value at a non-sampled point. This spatial correlation of the phenomena is represented by a variogram, which is a tool of geostatistics. The variogram function has to be estimated on the basis of the available data. In the case of a finite data set, the estimation of the variogram can be made for a finite set of vectors only. The variogram can be estimated with the help of the following formula using sample data [40]:

$$\gamma(h) = \frac{1}{2N(h)} \sum_{i=1}^{N(h)} [Z(x+h) - Z(x)]^2 \quad (1)$$

where γ (h) is the estimate of semi-variance, N (h) is the number of pairs observed [Z (X), Z (X+h)], and h is the distance between the pairs.

OK provides a single estimate at locations that minimizes the estimation variance and conditional bias [41]. OK is a spatial interpolation estimator $\hat{Z}$ (X_0) used to find the best linear unbiased estimate of a second-order stationary random field with an unknown constant mean as follows:

$$\tilde{Z}(X_{0)} = \sum_{i=1}^{n} \lambda_i \; Z(X_i) \quad (2)$$

where $\hat{Z}$ (X_0) is kriging estimate at a non-sampled location X_0; n is the number of measured value Z(X); Z(X_i) is the sampled value at location X_i; and λ_i is the weighting factor for Z (X_i). The estimation error is:

$$\tilde{\tilde{Z}}(X_{0)} - Z(X_0) = R(X_0) = \sum_{i=1}^{n} \lambda \; Z(X_i) - Z(X_0) \quad (3)$$

where Z (x_0) is the unknown true value at X_0; and R (X_0) is the estimation error. For an unbiased estimator, the mean of the estimation error must be equal to zero. Therefore,

$$\mathrm{E}\{\mathrm{R}(X_0)\} = 0 \quad (4)$$

and

$$\sum_{i=1}^{n} \lambda_i \; = 1 \quad (5)$$

The best estimator is always unbiased and has a minimum variance. The minimization of the estimation error variance under the constraint of unbiasedness leads to a set of simultaneous linear algebraic equations for the weighting factors, λ_i, which can be solved by an optimization routine and the method of Lagrange multipliers [38,42]. OK is also applied to estimate the block grades.

2.3.2. Cross Validation of Models and Validation of Estimation Results

Cross validation is a technique to check performance of the estimation methods [38]. This technique is based on omitting some sample points x_α from the set of variables Z (x) and then estimating them by kriging from the neighboring data Z (x_β), $\alpha \neq \beta$. Accordingly, at every sample point x_α, the Kriging estimate Z_α* and the associated Kriging variance $\sigma^2_{K\alpha}$ are calculated. Since the measured value Z_α = Z (x_α) is known, the empirical Kriging error (E_α) and standardized error (e_α) can be computed:

$$E_{\propto =} Z_{\propto}^{*} - Z_{\propto} \quad (6)$$

$$e_{\propto =} \frac{E_{\propto}}{\sigma_{K\alpha}} \quad (7)$$

Estimation model quality can be evaluated using the mean square standardized error with N data.

$$s = \frac{1}{N} . \sum_{\propto=1}^{N} e_{\propto}^{2} \quad (8)$$

The best fit for the model is the value closest to one [38]. Other indices such as the regression slope can be used to check the consistency of the selected neighborhood while cross-validating. In addition to the error variance and standardized error variance, examining the scatter plot of the estimated and true values is another possibility. These techniques show which model is more reliable. Estimation results can be validated in some applications if the real data are available. For instance, in mining studies, grade evaluations made on the basis of limited information (drill holes) can be validated by the real grades of the blocks [41].

2.3.3. Variography

Geostatistical estimations are based on the existence of a spatial structure in the data. Variography, or spatial statistics, is the most important means of showing the spatial correlation of sample values, which is computed by averaging the squared differences of grades between the pairs of samples that are a given distance apart [41]. Also, it is a very important study in the computerized resource estimation of the mining industry. The variogram is the function of the distance and direction separating the two locations that is used to measure the dependence. The variogram is described by a nugget, a sill, and a range parameter. The variogram is a quantitative descriptive statistic that can be graphically represented in a manner which characterizes the spatial continuity (i.e. roughness) of a data set.

The variogram models are widely used tools for spatial interpolation, which are the fundamental parameters for geostatistical modeling [43,44]. These models are fitted for different directions on the data set, which is used later on for the estimation of grade at a non-sampled location by OK method. To study the anisotropy of the ore deposit, variography was done in different directions and dips in the ore deposits.

2.4. Block modeling

One of the goals of this study is to create a block model for the iron ore deposit. An unconstrained block model was generated in a software and constrained by using the mineralized zone wireframes. The model composed of 3D cells or blocks, each of which has attributes such as grades. The model should be large enough to cover the full range of input data, which in most cases consist of one or more wireframes and drilling databases. 3D coordinates spatially define the model extents. To determine the extent of a block model, set the minimum coordinates of the starting blocks- the lowest angle, the south-west of the model, and the maximum block coordinates-the highest angle to the north-east of the model. This establishes space in the total area of impact that is used for estimating the grade and reserves. The sub-cells are not only helpful for accurate construction of a 3D grade model for the ore body, but also for identification of continuous sensitive differences of the ore grade in a single ore body [20]. The estimate of the grade of a block can be obtained as the linear average of the point estimates (e.g OK estimates).

Determination of a block size is the most important in the operation and selection of equipment at an open pit mine [45]. Also, choosing a suitable block size for evaluation of a reserve/resource is crucial for minimizing errors [7], because the choice of the block dimensions will affect the operation and mining costs. Mineral deposit mining decisions are based in part on the information provided in the grade block models obtained from samples [46]. The selection of such parameters is a complex engineering decision due to their great economic impact on the mining operation, as they will significantly affect the mine design and planning. In addition, several direct and indirect costs are associated with mining, and some costs such as drilling expenses differ depending on the block size [1]. Therefore, the costs can be reasonably reduced by determining the optimal size of the extracted blocks. To select the size of the block model, we should also consider several factors, such as the size of the blocks depend on the characteristics of the source, the size of the forms of bodies, type of ore, zonality, and length of sample analysis. The block size to be estimated must be comparative to the spacing of the available drilling information informing the estimate to avoid what is known as the “small block linear estimate problem” described by Stephenson and Vann, 2001 [47], which states that “as the block size decreases relative to drill spacing, the precision of the estimates decreases, often sharply”. Utilizing a larger block size will increase the averaging effect in the estimated block model in terms of concentrations of mineralized zones by smoothing of these points with high or low values within a large block [12,40,48-50]. Also, a smaller block size will show more details, but potentially more error in an anisotropic environment [48]. As a result, reducing the block size results in an increase in estimated errors (variance and standard deviation) for a final block model [48]. Therefore, it is necessary to select an optimal block size with respect to the deposit geometry and drilling pattern. In this research work, appropriate block size is determined using VIKOR method.

2.4.1. VIKOR Method

Use of multi-criteria decision-making (MCDM) methods are very useful as it allows simultaneous consideration of several criteria by taking into account the different relative importance attached to them [1]. The VIKOR is one the most robust techniques in MCDM problems that was established by [5], which is often used to solve discrete problems. The VIKOR method was developed for multicriteria optimization of complex systems. It determines the compromise ranking-list, the compromise solution, and the weight stability intervals for the preference stability of the compromise solution obtained with the initial (given) weights. This method focuses on ranking and selecting from a set of alternatives in the presence of conflicting criteria [51]. It aims to rank and weight different attributes under various criteria based on the introduction of multiple criteria ranking indices according to a particular measure of “closeness” to the “ideal solution” [51-53]. VIKOR model prioritizes or ranks the options via evaluation of the options on the basis of the criteria. In MCDM problems, the multi-disciplinary effective factors (here, diverse exploration and extraction data) are used to select the optimal block size and consequently to create block modeling of the iron ore deposit. VIKOR algorithm is adjusted based on the derived characteristics of exploration and extraction factors. The advantage of VIKOR is that the raw data can be used to evaluate the options as well as the expert opinion. In this research work, while introducing a comprehensive set of effective criteria to determine the appropriate block size, the best option (most appropriate size) for the C-North iron ore deposit is suggested using VIKOR method.

2.5. Grade-Tonnage Curve

Grade-tonnage curves are a visual representation of the impact of cut-off grades on mineral reserve. The tonnage and grade curves can be adjusted to account for several modifying factors to approximate or estimate the potentially mineable material available at various cut-off grades. Grade-tonnage curves are one of the tools which enable the mine managers to determine the correct long-term, mean-term and short-term parameters for ore production [5]. Drawing grade-tonnage curves is required in order to find the tonnage of different grades. According to assay data of each block, we could calculate the deposit based on different cut-off grades. The aim of the grade-tonnage calculation is to determine how much tonnes of metal is present in the deposit for the different grades of ore. It is calculated by the formula:

Grade-tonnage = Dx x Dy x Dz x T x n

where Dx, Dy, Dz = dimension of block in x, y, z directions, respectively, T= tonnes of ore per qubic meter of block (also called the tonnage factor), n= number of blocks

2.6. Classification of Reserve

Choosing the proper method for estimation of reserve with a minimum error is very important in geostatistical operations in mining engineering. One of the most important reasons for determining reserve classification is to justify the investment, which is especially important early in the life of the mine [54]. A useful classification is to consider categories A and B as equivalent to be measured, and category C1 as an indicated. C2 is then an inferred [32,55,56]. In this research, classification of the reserve has been carried out by relative estimation error variance method. In this method, with respect to apparent shape of relative estimation error variance histogram, the reserve is classified into measured, indicated and inferred categories. Relative estimation error variance is given below:

$$\sigma_R = \frac{\sigma_V}{Z_*^2} \tag{9}$$

where σ_R is the relative estimation error variance; σ_V: the block estimation error variance and Z_*^2 : the estimated grade of each block.

Several methods are utilized for classification of reserves and resources. The reserve is classified based on calculated estimation errors by JORC code. The classification framework is based on the code developed by the Joint Ore Reserves Committee of the Australian Institute of Mining and Metallurgy, Australian Institute of Geoscientists and Minerals Council of Australia [57]. This code is one of the international standards for mineral resource and ore reserve reporting, and it provides a template system that conforms to international society requirements [31,33].

2.7. Data Analysis

The present case study is based on an iron ore deposit located in the Sangan mining region. The strike of the deposit is almost along SE-NW. The study area covers 1.0 km^2 (1.0 × 1.0 km) and elevation ranges from 1409 m to 1745 m above sea level. The drill holes dataset plays an important role in both mineral exploration and grade estimation. The C-North iron ore deposit was explored by drilling 85 drill holes. The drill holes were spaced in an irregular grid pattern with a spacing of 20–100 m (average 50 m) between each drill hole. The depth of drill holes varies from 53.30 to 517.00 m, with an average depth of 234.15 m while total drilling depth is 19904.02 m. The iron ore is associated with seven different lithologies such as quartzite (QZIT), shale (SHAL), siltstone (SIST), skarn (SKAR), granite (GRAN), dacite (DACT), and rhyodacite (RD). A database was created based on the drill holes information which was collected from 85 drill holes in the C-North iron ore deposit. Drill hole data included concentrations of Iron (Fe (%)), Phosphorous (P (%)), and Sulfur (S (%)). The core logs were digitized using Microsoft Excel and were converted to a geological database, which included collar, survey and assay files. The main data used to create the geological model and the only data used for grade interpolation were the exploration drill hole data, consisting of assays and geological logging. The number of 3598 geochemical samples was collected from the drill holes and used for assays and logging in either 1.5 m or 2 m lengths. A composite length of 2.0

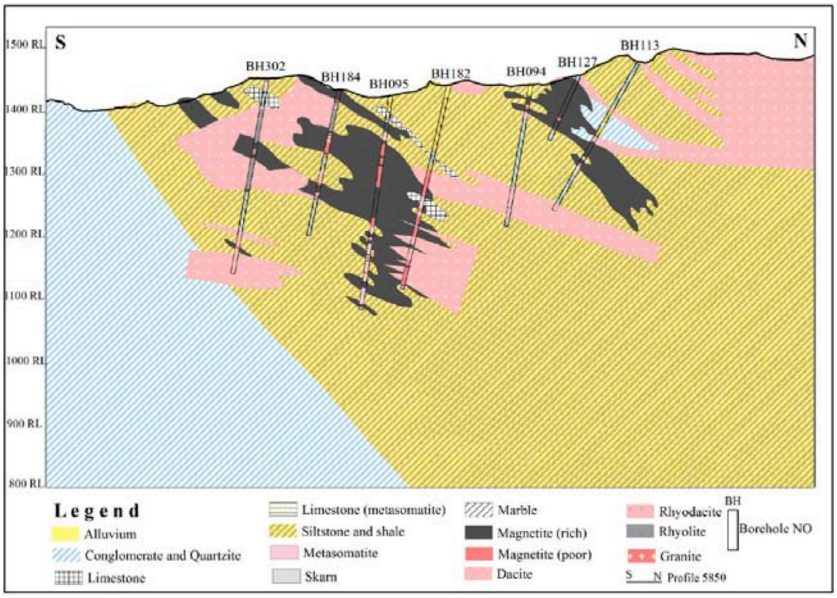

Figure 2: The geological cross-section line (5850) and the distribution of the ore zones in the C-North iron ore deposit [21].

meters was selected as it was the most prevalent interval length in the dataset [27].

Chemical analyses through ICP-MS method, are available for the major attributes Fe and SiO_2 as well as for minor attributes P and S. These measurements were assayed results used in the mine and production planning. Although Fe, SiO_2, P and S variables were analyzed, due to the importance of iron, only Fe content was chosen for geostatistical estimations of the ore deposit in the present study. It is noteworthy that phosphorous and sulfur content in the C-North iron ore are low. The drilling intersects various layers of sedimentary rocks, which are occasionally intercepted by intrusive. Five geological sections were selected in the north-south direction on the basis of sub-surface data at intervals of 50 and 100 meters (profiles number: 5850- 5950-6050-6100-6150) [27].

The shallowest drilling is 53.3 m (BH.219) and the deepest drilling is 517 m (BH.59) deep. In order to observe the spatial distribution modeling in 2D, one cross-section line (profile number: 5850) is drawn containing the drill holes that take place in the ore zone areas (Figure **2**). The interpretation of the ore zones was based on geological control on the mineralization. In this cross-section, the distribution of the ore zones is observed between BH.113 and BH.94 drill holes and between BH.182 and BH.302 drill holes at levels of about 1200–1400 m and 1100- 1400 m, respectively [27]. This stage consists of an exploratory study and variogram analysis of a real dataset (sample assays from exploration drill holes) from C-North iron ore deposit.

2.7.1. Basic Statistics

Statistical studies and spatial analysis were performed on the raw data of the drill holes and the results of the basic statistical parameters and frequency distribution (histogram) of the primary iron grade are shown in Figure **3** [58]. The grade distribution of the iron concentrations is not normal. The histogram shows that the data are having multiple populations, and is negatively skewed (Figure **3**). The iron grade (Fe%) as a regionalized variable has no trend in any direction; this means that the Fe concentration does not depend on the coordinates of the samples (Figure **4a-c**). Consequently, assumptions of the stationary function are tenable.

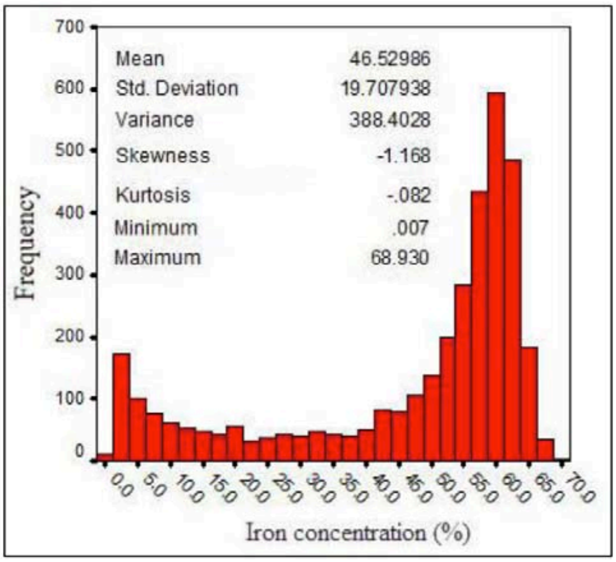

Figure 3: Histogram showing grade distribution of Fe (%) in the drill hole samples of the study area.

After exploration data analysis, the spatial continuity was investigated by constructing variogram models. In the spatial studies, both directional and non-directional variograms were constructed. The directional variogram model provided a better understanding of the deposit and enabled to check for anisotropies. The

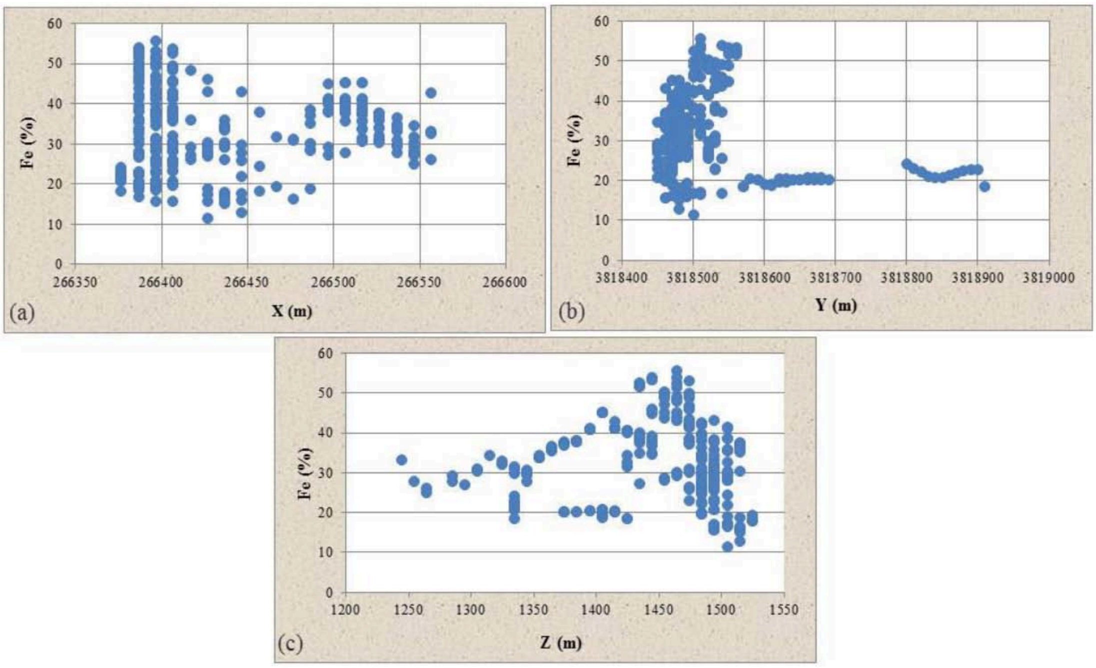

Figure 4: Scatter plots for variability of Fe concentration in (**a**) east- west (X) direction, (**b**) north-south (Y) direction, and (**c**) depth (Z) of mineralization level in the study area.

presence of anisotropy was taken into account during ordinary kriging. The non-directional and directional variograms were generated by Datamine Studio software in the C-North iron ore deposit, as shown in Table **1** and Figure **5**. Both the variograms show a very good spatial structure with fitted models. Three main directions of the search ellipsoid were chosen from the experimental directional variograms of Fe to create the best variography model for the OK estimation. In the study area, structural features include the major faults and fault zones along the axial plane. Iron behaves differently in relation to these structural features. The main structures of the study area, in agreement with the obtained variograms and the main mineralization trends.

One of the methods to check the validity of the results of estimation is cross-validation. In order to evaluate the accuracy of the variogram model (fitted model), each one of the grade values was estimated using the data from the neighborhood. The scatter-plot between the real and the estimated grades are represented in Figure **6**. The correlation coefficient between the estimated points and known points was 0.71.

3. DISCUSSION

In the mineral industry, the information available for modeling is limited and represents a very small fraction of the domain of interest. In this study, grade estimation of the iron ore deposit has done using the OK method. Based on geostatistical parameters, the suitable size of blocks is half of the distance between exploratory drilling networks. For size optimization of mining blocks, first the block model of deposit was constructed using 2.5, 5, 7.5, 10, 12.5 and 15 m blocks by modeling program. Using the kriging method and based on variogram parameters, the grade of various deposit blocks was then determined. In addition to the geostatistical parameters, the extraction parameters are important in choosing the optimum block size. Generally, the most important factors affecting the dimensions of the blocks are cost, and product price. In this study, six additional criteria, including safety, environmental impact, productivity, capacity of machinery, capital costs and operating costs have been considered. Table **2** shows the characteristics of nine most effective factors used in this study to determining the size of the blocks. C1 to C3 criteria are quantitative criteria and various numerical values and

Table 1: Parameters of the Spherical Non-Directional and Directional Variogram Models of the Study Area

Structure/ variables	Range (m)	Sill $(\%)^2$	Nugget effect	C-value
Non-direction	422.1	144.2	97.3	46.9
1	104.8	120.08	90.07	30.01
2	41.01	116.2	53.7	62.5
3	308.73	157.01	88.7	68.31

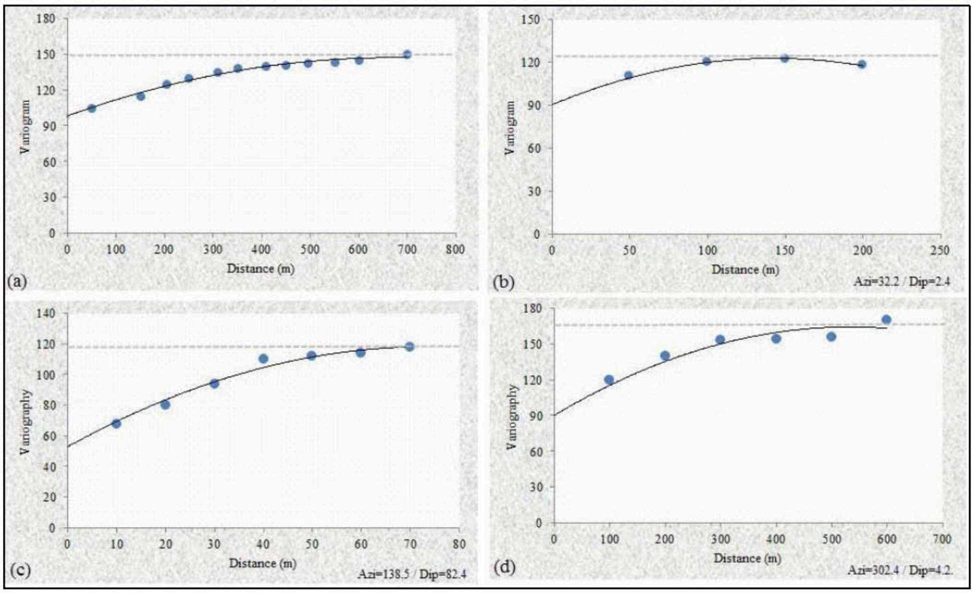

Figure 5: Non-directional and directional variograms (with appropriate fitted model) of the study area: **a**) non-directional, **b**) directional with Azimuth = 32.2 degree; Dip = 2.4 deg, **c**) directional with Azimuth = 138.5 degree; Dip = 82.4 deg, **d**) directional with Azimuth = 302.4 degree; Dip = 4.2 deg.

some calculations have been used for their estimation. Other criteria are qualitative and expert opinion has been used to determine their values for different options (different block sizes). In criteria with a positive impact, the higher the value of these criteria for an option, the higher preference of that option. In criteria with a negative impact, the increasing value of these criteria for an option reduces the preference of that option for selection. This research work is conducted on selecting the appropriate size of the mining blocks using VIKOR method.

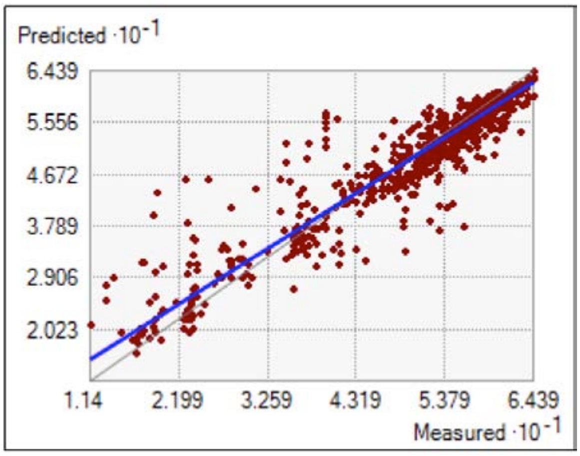

Figure 6: Cross-validation diagram to evaluate accuracy of real and estimated (kriged) values of Fe in the C-North ore deposit.

At this stage, according to the proposed dimensions for block size, six sizes including 2.5 m (A1), 5 m (A2), 7.5 m (A3), 10 m (A4), 12.5 m (A5) and 15 m (A6) were selected as six options (alternatives) based on the nine effective criteria, including C1 to C9 and the decision matrix was formed to choose the proper size for mineral block in Angouran mine.

As noted above, C1, C2 and C3 are quantitative criteria and their values for various options have been determined on the basis of detailed calculations. Other criteria are qualitative and expert opinions that have been used to determine their values for different options. Thus, the decision matrix was determined. Eigenvector technique was used to determine the relative importance of the criteria. For this purpose, paired comparison matrix of the criteria was formed through the survey of expert opinion on the relative importance of the criteria in accordance with whole time. In the end, while calculating the geometric mean of data in each row, the geometric mean obtained in each row was divided by the sum of geometric mean elements to normalize the data (i.e. making the sum of weights equal to 1). In this method, the final normalized weight of each criterion (also known as eigenvector) was obtained.

After determining the decision matrix and relative importance of the criteria, other steps of VIKOR

Table 2: Effective Criteria in Determining the Appropriate Size of Blocks

Criterion	t estimator	Standard deviation (%)	Mean (%)	Safety	Environmental impact	Productivity	Production capacity of machinery	Capital costs	Operational costs
Sign	C_1	C_2	C_3	C_4	C_5	C_6	C_7	C_8	C_9
Aspect	Positive	Negative	Positive	Negative	Negative	Positive	Negative	Positive	Negative

Table 3: Determining the Ideal Negative and Positive Points

f^*	0.4069	0.4021	0.4117	0.6103	0.0795	0.6321	0.7925	0.0843	0.0742
f^-	0.4016	0.4142	0.3938	0.0721	0.6223	0.0832	0.0642	0.7106	0.5957

Table 4: Satisfaction, Rejection and VIKOR Indexes for Alternatives

Alternatives	S_i	R_i	Q_i
A_1	0.4326	0.1124	0.8867
A_2	0.6038	0.2224	0.4986
A_3	0.6234	0.2167	0.2235
A_4	0.6774	0.3546	0.0095
A_5	0.3765	0.1223	0.9945
A_6	0.4956	0.2406	0.3889

method to choose the optimum size of blocks are described below. First, the normal decision matrix was defined and then the weighted normal matrix was obtained by multiplying the normal matrix elements by relative importance of the criteria. In the end, while determining the positive and negative ideal points in the normal weight matrix (Table **3**) and satisfaction index, the rejection and VIKOR indexes are calculated (Table **4**).

Finally, the options were arranged based on the values of Q, R, S in three groups from small to large. The best option is the one with the smallest Q, so the fourth option (10×10×10 meters) was recommended as the optimal size for mining blocks in the C-North ore deposit.

An exploratory analysis and geostatistical modeling of the grades assayed on a set of drill hole samples was performed, which allowed constructing a grade block model. A geological cut-off grade of 20 % Fe was determined from the classical statistical analysis of the data for the C-North iron ore deposit. This was used as a trigger value to create grade composites for interpretation. Geological data were used to assist in interpretation of the mineralized envelopes. Interpretation and wireframing was then carried out for all mineralized envelopes over twenty cross-sections. A three dimensional block model of the C-North iron ore deposit was prepared in Datamine software on using the ore body block size of 10 m (X) × 10 m (Y) × 10 m (Z). The block model was estimated by using the Ok method in the same block support (10mN x 10mE x 10mRL) after adding to the dataset the iron grade values provided by samples from the drill holes. A study was taken up to evaluate the grade distribution of a magnetite iron ore deposit. The iron ore deposit is characterized by rugged and undulating topography. The main mineralization in the C-North deposit has a SE-NW trend with moderate to steep south easterly slope and a strike length of 1000 m with a width varying between 600 and 1000 m.

Due to the importance of iron, Fe content was selected as a regional variable and geostatistical estimations were carried out for this variable. The block model contains 47,349 blocks with a block size of 10 × 10 × 10 m, including the ore and waste blocks. Grade blocks were created for identification of the waste (W), low grade (LG) and high grade (HG) areas. The deposit has a high grade of Fe content. Grade maps show that the deposit broadly can be distributed into three classes depending on the estimated Fe grade. It is also inferred that the high grade part of the ore body has very high grade (> 45 %) of Fe, the medium grade (35-45 % Fe) and low grade (20- 35 % Fe) (Figures **7** and **8**). Based on the results of the 3D models obtained by the OK estimation method, parts with Fe values

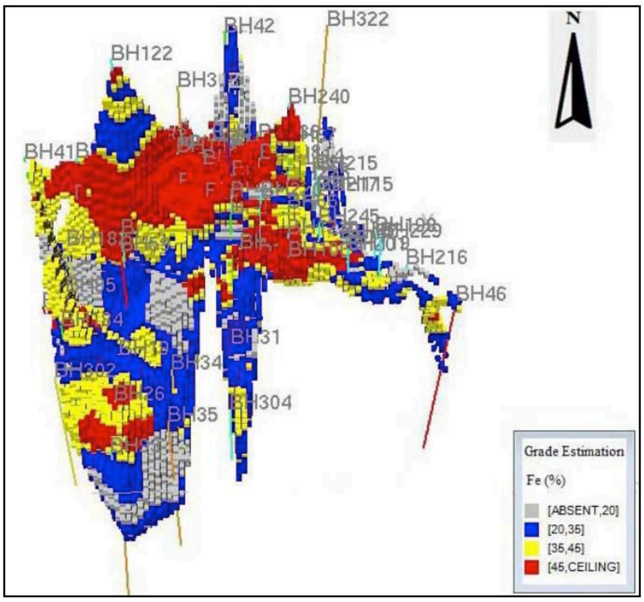

Figure 7: 3D model of estimations of Fe grade by OK method in the C-North ore deposit (view to the north).

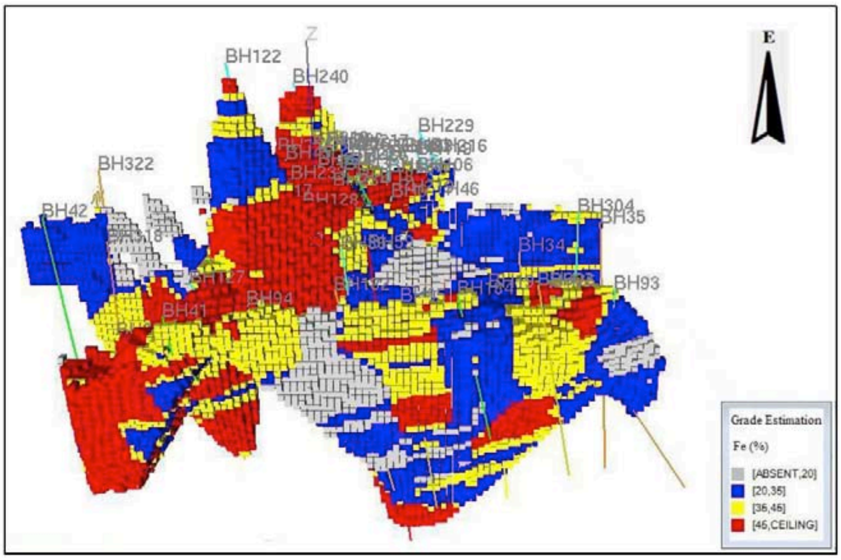

Figure 8: Ordinary kriged block model showing Fe grades in the C-North ore deposit (view to the east).

higher than 45% (high-grade mineralized zones) occur in the northern parts of the study area with an E-W trend.

The ordinary kriged model was checked locally in section to determine if the original sample grades were reflected in the block model grades. The process involved averaging both the blocks and the samples in panels of 10 m (easting) by 10 m (northing) by 10 m (RL) for the C-North deposit. The grades were calculated from the individual estimated blocks and composite assay dataset in the C-North ore deposit. Local validation of the OK block model with the original drill hole sample values for Fe is shown in Figure **9**. It can be seen that there is a high correlation between the original sample grades and the ordinary kriging interpolated block model grades. Generally, a good agreement is observed between the data and block model mean grade for all variables for easting, northing and RL slices. For average grade conformance, all domains in low grades and high grades display comparable performance relative to the data.

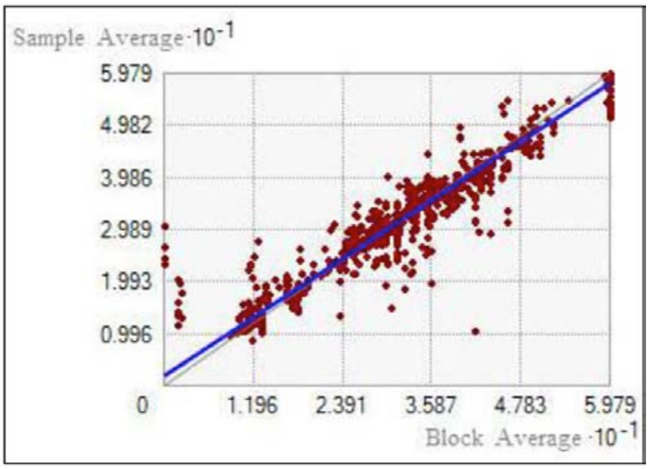

Figure 9: Fe estimate validation plot in 10 m×10 m×10 m panels (RL).

The grade-tonnage curve of the block model in the C-North iron ore deposit has been estimated at several cut-off grades with the OK result of the respective model. The grade- tonnage curve for the C-North iron ore deposit is generated for different assays, as illustrated in Figure **10**. The total tonnage of the ore deposit based on various cut-off grades is different and with 20% cut-off grade are 116 million tones, with 25% cut-off grade are 106 million tones and with 30% cut-off grade are 95 million tones. It could be seen that in the cutoff grade of high values, the tonnage of the reserve was reduced and the Fe values of reserves are increased.The grade-tonnage curve provides two key characteristics for the deposit under investigation. Firstly, the blue line represents the cumulative tonnage (y1-axis) of all blocks with the grade at or above the selected cut-off grade (x-axis) (Figure **10**). As one might intuitively expect, the tonnage drops as the cut-off grade is increased and the tonnage increases as the cut-off is decreased. Secondly, the red line represents the average grade (y2-axis) of all the blocks with grade at or above the selected cut-off grade (x-axis). Based on a grade-tonnage curve, possible resource has been estimated for this deposit. Using a 20% cut-off, this resource would be contained 116 Mt at an average grade of 23%. Figure **11** shows grade–tonnage relationship for Fe grades above 35 % in the C-North iron deposit. As the criteria for ore classification becomes more selective, the tonnage above the cut-off grade of the deposit decreases. Conversely, as the cut-off grade is lowered, the tonnage of the deposit increases.

In this research work, the reserves were classified based on the relative estimation error variance and the JORC standard. In this section, classification of the reserve has been carried out by relative estimation error variance method. The Resource has been

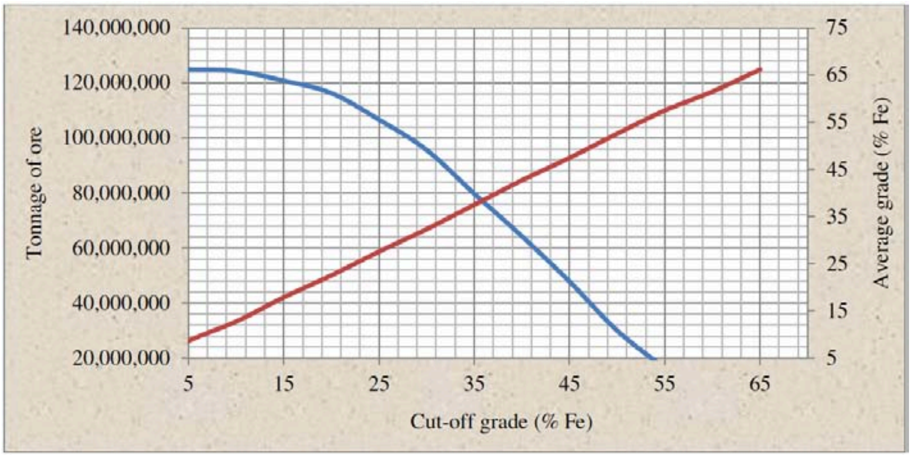

Figure 10: Curve of grade-tonnage in the C-North iron ore deposit.

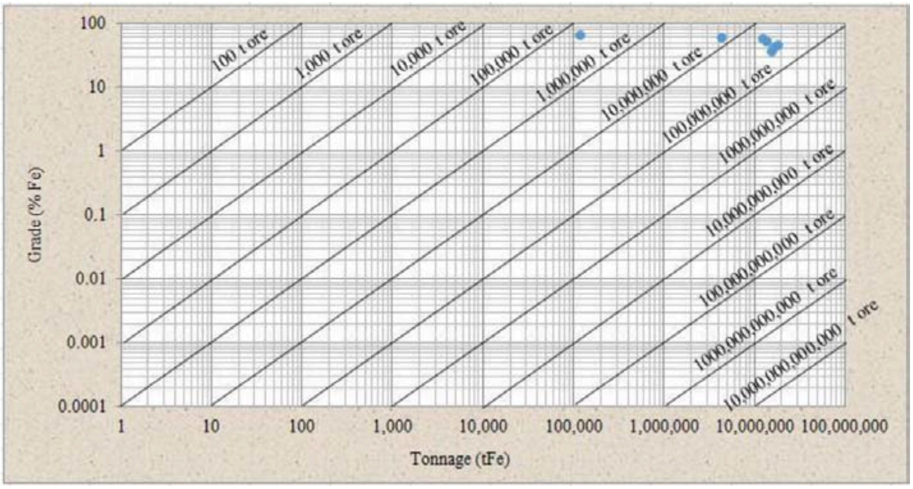

Figure 11: Grade-tonnage relationship for Fe grades above 35 % of the C-North iron ore deposit.

Table 5: Result of Reserve Classification using Relative Estimation Error Variance Method in the C-North Iron Ore Deposit

Error	Reserve category	Tonnage (ton)
0-10 %	Measured	82,156,000
10-20 %	Indicated	93,587,000
20-30 %	Inferred	115,989,000

classified as measured, indicated, and inferred. Table **5** shows the results of reserve classification using the relative estimation error variance method in the C-North iron ore deposit.

Also, the C-North ore deposit has been classified based on the calculated estimation errors by JORC code as shown in Table **6** [55]. Results obtained by OK methods were validated by statistical methods (Figure **12**). Most estimated blocks by OK method have low values of errors, which are lower than 20 %. Resource classification is based on confidence in the geological domaining, drill spacing and geostatistical measures.

Table 6: Result of Reserves Classification Based on JORC Standard in the C-North Iron Ore Deposit

Error	Average grade (%)	Tonnage (%)	Classification
0-20 %	41.86	99.63	A
20-40 %	23.15	0.21	B
40-60 %	20.32	0.16	C
> 60 %	-	-	Possible

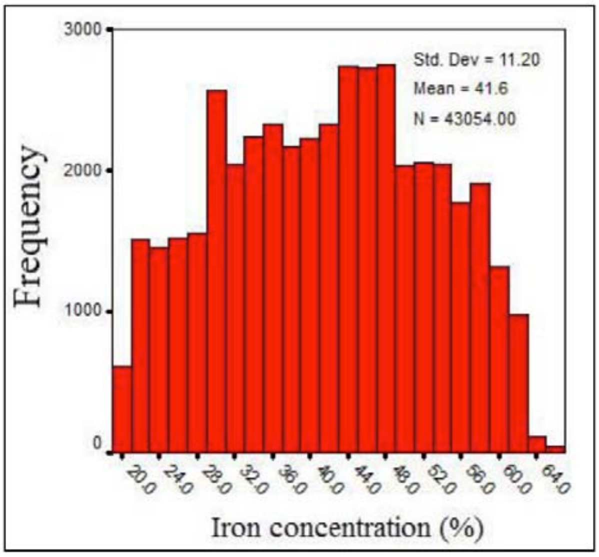

Figure 12: Histogram of estimated data for Fe grades above 20% by OK method.

4. CONCLUSIONS

In the present study, an attempt has been made for estimation of the iron ore resource based on the linear geostatistical estimation method in the Sangan mining region, NE Iran. This research work focuses on the generation of an ore block model and grade interpolation of the C-North iron ore deposit that had been estimated by the OK method using variogram model to evaluate the deposit, with the help of geostatistical methods. Fe content was chosen as a regionalized variable for grade estimation. Based on the basic statistical analysis from 85 drill holes, histogram plot of the present data showed that there is the presence of multiple populations. For the purpose of block modeling, according to the results of the VIKOR method for optimal block size, the deposit was discretized into various blocks with the size of each block being 10m × 10m × 10m. OK was used to estimate 3D blocks. A total number of 47,349 blocks were recorded in the study area. Grade blocks were created for the identification of the waste (< 20% Fe), low grade (20- 35 % Fe), medium grade (35- 45 % Fe), and high grade (> 45% Fe) areas. The estimated iron values of the respective blocks were compared with the nearest possible drill holes analysis data while all blocks within the domains were correctly estimated. The main mineralization in the C-North deposit has a SE-NW trend with moderate to steep south easterly slope. Iron grade maps indicate that there is significant structural control on the ore grade distribution. Structural features played an important role in the concentration of the metals and upgrading of the ore deposit. The grade-tonnage curve of the block model in the C-North iron ore deposit had been estimated at several cut-off grades with the OK result of the respective model. Based on grade-tonnage curve, possible resource has estimated for this deposit. Using a 20% cut-off, this resource would be contained 116 Mt at an average grade of 23% Fe. The reserves were classified based on the relative estimation error variance and the JORC standard. The resource is estimated as 83 million tons at average grade of 41.86 % Fe by OK method from the block model developed by mine planning software. Users of this visualization system can find that its strengths lie in the simplicity of complex deposit modeling and the increased availability of important information in 3D space.

ACKNOWLEDGMENTS

The authors would like to thank the Amirkabir University of Technology (Polytechnic Tehran), Iranian Mines and Mining Industries Development and Renovation Organization (IMIDRO), and Sangan Iron Ore Mines (SIOM) for supporting this research (Project NO.9512526). The contributions of Adonis Fard Mousavi, Samira Rezaei, and Nima Jabbari are highly appreciated.

REFERENCES

[1] Hayati M, Rajabzadeh R, Darabi M. Determination of Optimal Block Size in Angouran Mine Using VIKOR Method. J Mater Environ Sci 2015; 6: 3236-3244.

[2] Kameshwara R, Raghavendra R, Chinna Allu N. Assessing grade domain of iron ore deposit using geostatistical modelling: A case study. Journal of the Geological Society of India 2014; 83: 549-554. https://doi.org/10.1007/s12594-014-0082-6

[3] Choudhury S. Comparative Study on Linear and Non-Linear Geostatistical Estimation Methods: A Case Study on Iron Deposit. Development for Mining of Mineral and Fossil Energy Resources 2015; 131-139. https://doi.org/10.1016/j.proeps.2015.06.017

[4] Hustrulid W, Kuchta M. Open Pit Mine Planning and Design, Taylor & Francis, ISBN 9780415407410, USA 2006.

[5] Daya AA. Reserve estimation of central part of Choghart north anomaly iron ore deposit through ordinary kriging method. International Journal of Mining Science and Technology 2012; 22: 573-577. https://doi.org/10.1016/j.ijmst.2012.01.022

[6] Shademan khakestar M, Hassani H, Moarefvand P. Determining the best search neighbourhood in reserve estimation, using geostatistical method: A case study anomaly No. 12A iron deposit in central Iran. Journal of the Geological Society of India 2013; 81: 581-585. https://doi.org/10.1007/s12594-013-0074-y

[7] Shahbeik S, Afzal P, Moarefvand P, Qumarsy M. Comparison between ordinary kriging (OK) and inverse distance weighted (IDW) based on estimation error. Case study: Dardevey iron ore deposit, NE Iran. Arab J Geosci 2014; 7: 3693-3704. https://doi.org/10.1007/s12517-013-0978-2

[8] Mery N, Emery X, Cáceres A, Ribeiro D, Cunha E. Geostatistical modeling of the geological uncertainty in an iron ore deposit. Ore Geology Reviews 2017; 88: 336-351. https://doi.org/10.1016/j.oregeorev.2017.05.011

[9] Tahernejad MM, Khalokakaie R, Ataei M. Analyzing the effect of ore grade uncertainty in open pit mine planning; a case study of the Rezvan iron mine, Iran. International Journal of Mining and Geo-Engineering 2018; 1: 53-60.

[10] Kim S, Choi Y, Park H. New Outlier Top-Cut Method for Mineral Resource Estimation via 3D Hot Spot Analysis of Borehole Data. Minerals 2018; 8: 348. https://doi.org/10.3390/min8080348

[11] Tutmez. An uncertainty oriented fuzzy methodology for grade estimation. Computers and Geosciences 2003; 33: 280-288. https://doi.org/10.1016/j.cageo.2006.09.001

[12] David M. Geostatistical Ore Reserve Estimation, Elsevier, Amsterdam 1970.

[13] Boisvert JB, Ortiz JM, Deutsch CV. Local recoverable reserves prediction with block LU simulation. International Journal of Mining and Mineral Engineering 2008; 1: 3-21. https://doi.org/10.1504/IJMME.2008.020454

[14] Tahmasebi P, Hezarkhani A. Application of adaptive neuro-fuzzy inference system for grade estimation; case study, Sarcheshmeh porphyry copper deposit, Kerman, Iran. Australian Journal of Basic and Applied Sciences 2010; 4: 408-420.

[15] Martins AC, Nader B, De Tomi G. A novel application of cellular automata for the evaluation and modelling of mineral resources. International Journal of Mining and Mineral Engineering 2011; 3: 303-315. https://doi.org/10.1504/IJMME.2011.045472

[16] Journel AG, Huijbregts CJ. Mining geostatistics. Academic press 1978; 600.

[17] Brown WM, Gedeon TD, Groves DI, Barners RG. Artificial networks: a new method for mineral prospectivity mapping. Australian Journal of Earth Sciences 2000; 47: 757-770. https://doi.org/10.1046/j.1440-0952.2000.00807.x

[18] Harris JR, Grunsky E. Predictive lithological mapping of Canada's north using random forest classification applied to geophysical and geochemical data. Computers & Geosciences 2015; 88: 9-25. https://doi.org/10.1016/j.cageo.2015.03.013

[19] Haldar SK. Mineral Exploration: Principles and Applications. Elsevier Science Publishing Co Inc, United States 2013.

[20] Wang G, Huang L. 3D geological modeling for mineral resource assessment of the Tongshan Cu deposit, Heilongjiang Province, China. Geoscience Frontiers 2012; 3: 483-491. https://doi.org/10.1016/j.gsf.2011.12.012

[21] Rezaei A, Hassani H, Moarefavand P, Golmohammadi A. Determination of unstable tectonic zones in C–North deposit, Sangan, NE Iran using GPR method: Importance of structural geology. Journal of Mining and Environment 2019; 10: 177-195.

[22] Sepidbar F, Mirnejad H, Mi C. Mineral chemistry and Ti in zircon thermometry: Insights into magmatic evolution of the Sangan igneous rocks, NE Iran. Journal of Chemie Der Erde 2018; 78(2): 205-214. https://doi.org/10.1016/j.chemer.2018.02.001

[23] Malekzadeh Shafaroudi A, Karimpour MH, Golmohammadi A. Zircon U–Pb geochronology and petrology of intrusive rocks in the C-North and Baghak districts, Sangan iron mine, NE Iran. Journal of Asian Earth Sciences 2013; 64: 256-271. https://doi.org/10.1016/j.jseaes.2012.12.028

[24] Golmohammadi A, Karimpour MH, Malekzadeh Shafaroudi A, Mazaheri SA. Alteration-mineralization, and radiometric ages of the source pluton at the Sangan iron skarn deposit, northeastern Iran. Ore Geol Rev 2015; 65: 545-563. https://doi.org/10.1016/j.oregeorev.2014.07.005

[25] Kermani A, Forster H. Petrography, Mineralogical and geochemical investigations of the Sangan Iron ore deposit, northeastern Iran. Proceedings of Third Mining Symposium of Iran 1991.

[26] Mazhari N, Malekzadeh Shafaroudi A, Ghaderi M, Star Lackey J, Lang Farmer G, Karimpour MH. Geochronological and geochemical characteristics of fractionated I-type granites associated with the skarn mineralization in the Sangan mining region, NE Iran 2017. https://doi.org/10.1016/j.oregeorev.2017.01.003

[27] Rezaei A, Hassani H, Moarefvand P, Golmohammadi A. Modeling the effect of Structural Pattern on Mineralization in Sangan Central Iron Ore Mine, Iran. PhD Thesis, Amirkabir University of Technology (AUT), Tehran, Iran 2019; p. 364.

[28] Fauvelet E, Eftekhar-Nezhad J. Explanatory text of the taybad quadrangle map1: 250000, Geological Survey of Iran 1990.

[29] Rezaei A, Hassani H, Moarefvand P, Golmohammadi A. Lithological mapping in Sangan region in Northeast Iran using ASTER satellite data and image processing methods. Journal of Geology, Ecology and Landscapes 2020; 4(1): 59-70. https://doi.org/10.1080/24749508.2019.1585657

[30] Rezaei A, Hassani H, Moarefvand P, Golmohammadi A. Investigation the Effect of Structural Pattern on Mineralization Model In the C-North Ore Deposit, Sangan, NE Iran. Journal of Mineral Resources Engineering (JMRE) 2019; 4(2): 1-5. https://doi.org/10.1080/24749508.2019.1585657

[31] Li X, Xie Y, Guo Q, Li L. Adaptive ore grade estimation method for the mineral deposit evaluation. Mathematical and Computer Modelling 2010; 52: 1947-1956. https://doi.org/10.1016/j.mcm.2010.04.018

[32] Isaaks EH, Srivastava RM. An Introduction to Applied Geostatistics. Oxford University Press, New York, USA 1989.

[33] Asghari O, Madani Esfahani N. A new approach for the geological risk evaluation of coal resources through a geostatistical simulation. Case study: Parvadeh III coal deposit. Arab J Geosci 2013; 6: 957-970.

[34] Monjezi M, Rajabalizadeh Kashani M, Ataei M. A comparative study between sequential Gaussian simulation and kriging method grade modeling in open-pit mining. Arab J Geosci 2013; 6: 123-128. https://doi.org/10.1007/s12517-011-0293-8

[35] Krige DGA. Statistical Approach to Some Mine Valuations and Allied Problems at the Witwatersrand. Master's Thesis, University of Witwatersrand, Johannesburg, South Africa 1951.

[36] Armstrong M. Basic Linear Geostatistics; Springer: Berlin/Heidelberg, Germany 1998; 15-115. https://doi.org/10.1007/978-3-642-58727-6_2

[37] Bertoli OJ. Quantitative Kriging Neighbourhood Analysis for the Mining - A Description of the Method with Worked Case Examples. Bendigo, Vic: 5th International Mining Geology Conference 2003.

[38] Chilès JP, Delfiner P. Geostatistics: Modeling Spatial Uncertainty, Wiley, New York 2012. https://doi.org/10.1002/9781118136188

[39] Pokhrel RM, Kuwano J, Tachibana S. A kriging method of interpolation used to map liquefaction potential over alluvial ground. Engineering Geology 2013; 152: 26-37. https://doi.org/10.1016/j.enggeo.2012.10.003

[40] Deutsch CV, Journel AG. GSLIB: Geostatistical Software Library and User's Guide. 2nd ed. Oxford University Press, New York 1998; 369.

[41] Matheron G. Principles of Geostatistics. Econ Geol 1963; 58: 1246-1266. https://doi.org/10.2113/gsecongeo.58.8.1246

[42] Hu H, Shu H. An improved coarse-grained parallel algorithm for computational acceleration of ordinary Kriging interpolation. Computers and Geosciences 2015; 78: 44-52. https://doi.org/10.1016/j.cageo.2015.02.011

[43] VerHoef JM, Cressie N. Multivariable spatial prediction. Math Geol 1993; 252: 219-239. https://doi.org/10.1007/BF00893273

[44] Calder CA, Cressie N. Kriging and variogram models. Elsevier, Oxford 2009; 49-55. https://doi.org/10.1016/B978-008044910-4.00461-2

[45] Jara RM, Couble A, Emery X, Magri EJ, Ortiz JM. Block size selection and its impact on open-pit design and mine planning. The Journal of The South African Institute of Mining and Metallurgy 2006; 106: 205-212.

[46] Araújo, Cristina da Paixão, Costa, João Felipe Coimbra Leite, Koppe, Vanessa Cerqueira. Improving short-term grade block models: alternative for correcting soft data. REM - International Engineering Journal 2018; 71(1): 117-122. https://doi.org/10.1590/0370-44672016710007

[47] Stephenson PR, Vann J. Common Sense and Good Communication in Mineral Resource and Ore Reserve Estimation, in Mineral Resource and Ore Reserve Estimation – The AusIMM Guide to Good Practice (Ed: A C Edwards), (The Australasian Institute of Mining and Metallurgy: Melbourne) 2001; 13-20.

[48] Journel A. Geostatistics: roadblocks and challenges, in A. Soares, ed, Geostatistics-Troia 1993; 1: 213-224. https://doi.org/10.1007/978-94-011-1739-5_18

[49] Emery X. Simple and ordinary kriging, multi-gaussian kriging for estimating recoverable reserves. Mathematical Geology 2005; 37: 295-319. https://doi.org/10.1007/s11004-005-1560-6

[50] Emery X, Ortiz JM. Two approaches to direct block-support conditional co-simulation. Computers & Geosciences 2011; 37: 1015-1025. https://doi.org/10.1016/j.cageo.2010.07.012

[51] Opricovic S, Tzeng GH. Compromise solution by MCDM methods: A comparative analysis of VIKOR and TOPSIS. European Journal of Operational Research 2004; 156: 445-455. https://doi.org/10.1016/S0377-2217(03)00020-1

[52] Opricovic S. Multicriteria Optimization of Civil Engineering Systems, Faculty of Civil Engineering, Belgrade 1998.

[53] Abedi M, Mohammadi R, Norouzi GH, Mohammadi MSM. A comprehensive VIKORmethod for integration of various exploratory data in mineral potential mapping. Arab J Geosci 2016; 9: 482. https://doi.org/10.1007/s12517-016-2512-9

[54] Michel D. Geostatistical ore reserve estimation. New York: Elsevier Scientific Publishing Co. 1982.

[55] Snowden DV. Practical interpretation of resource classification guidelines. In: AusIMM Annual Conference, Perth 1996.

[56] Dowd PA. A review of recent developments in geostatistics. Comput Geosci 1992; 17: 1481-500. https://doi.org/10.1016/0098-3004(91)90009-3

[57] JORC. Australasian Code for Reporting of Identified Mineral Resources and Ore Reserves (The JORC Code). The Joint Ore Reserves Committee of the Australasian Institute of Mining and Metallurgy, Australian Institute of Geoscientists, and Minerals Council of Australia 2012.

[58] Rezaei A, Hassani H, Tziritis E, Fard Mousavi SB, Jabbari N. Hydrochemical characterization and evaluation of groundwater quality in Dalgan basin, SE Iran. Journal of Groundwater for Sustainable Development 2020; 10: 2352-801X, 1-13. https://doi.org/10.1016/j.gsd.2020.100353

Received on 30-11-2019 Accepted on 21-12-2019 Published on 27-12-2019

DOI: https://doi.org/10.15377/2409-5710.2019.06.4